Effect of HIPping, stress and surface finish on the environmental degradation of Y-TZP ceramics

K. L. GRANT*, R.D. RAWLINGS, R. SWEENEY
Department of Materials, Imperial College of Science, Technology and Medicine, London, SW7 2BP, UK
E-mail: karen.grant@agresearch.co.nz, r.rawlings@ic.ac.uk, richard.sweeney@ic.ac.uk

Hot isostatically pressed (HIPped) and hot pressed (designated unHIPped) bar samples of yttria stabilized tetragonal zirconia polycrystalline ceramic (3Y-TZP) were subjected to three point bend testing in water at 90 °C. HIPped femoral heads with three different surface finishes were also aged in 90 °C water. The early stages of the environment induced tetragonal to monoclinic transformation was monitored as a function of time by X-ray diffraction, white light interferometry and scanning electron microscopy. HIPped samples were found to transform less readily than unHIPped samples and have a longer incubation period prior to transformation. There was an increase in the amount of monoclinic phase detected following the application of stress, particularly on the compression surface. Microcraters, believed to result from the expulsion of transformed grains when stress was applied, were observed on tension surfaces, particularly of unHIPped samples. There was no effect of surface roughness on the environment induced transformation for the range of surface finishes investigated.

1. Introduction

The outstanding room temperature strength and toughness of tetragonal zirconia polycrystalline ceramics (TZPs) is due to transformation toughening, whereby the metastable tetragonal zirconia transforms to the equilibrium monoclinic phase at the crack tip [1]. The transformation is associated with a 3% volume expansion causing an effective back stress that hinders crack propagation [2].

Tetragonal zirconia is obtained at room temperature by the judicious addition of stabilizing oxides, such as yttria, and maximizing the elastic constraint of the surrounding matrix by minimizing the grain size. Thus yttria stabilized TZPs typically contain 3 mol % yttria (designated 3Y-TZP) and have submicron grains [3].

Unfortunately, it has been found that the tetragonal to monoclinic transformation in 3Y-TZP can occur at the surface when the ceramic is held in an aqueous environment at an elevated temperature [4–6]. There are numerous investigations that have shown that this uncontrolled surface transformation is accompanied by a degradation in mechanical performance.

A previous investigation by two of the authors of the microstructural aspects of the environmentally induced transformation in HIPped femoral heads aged at 134 °C and 2 bars demonstrated that the nucleation and growth rates were constant with time [7]. Good agreement was found between the prediction of the percentage monoclinic formed as a function of time obtained by inserting these values into the Johnson-Mehl-Avrami equation with a time exponent of 4 and the curve produced using X-ray diffraction data. Similar conclusions have been drawn by Chevalier *et al*. [8].

In spite of this problem, due to the good mechanical performance and wear resistance of 3Y-TZP, it has recently been used for the femoral head in some hip prostheses. The highest quality material (high purity, fine-grained) is employed and although the environment is aqueous, the temperature is only 37 °C. Nevertheless, this component would be expected to be suitable for a service life in excess of 15 years. Early work on what would now be considered low quality material showed a slight increase in monoclinic content after 19 months aging in Ringer's solution at body temperature [9]. In contrast, an investigation of explanted femoral heads following two to three years in the physiological environment showed no transformation or degradation in mechanical properties [10]. It would appear the current generation of 3Y-TZP may be suitable for biomedical applications, but nevertheless a better understanding of the degradation process would assist future development. Furthermore, in the general context, there is no doubt that the environment induced degradation is the major factor hindering the wider application of 3Y-TZPs.

There is a dearth of information in literature on the effects of processing method, surface finish and stress on

*Now at Ruakura Research Centre, East Street, Private Bag 3123, Hamilton, NZ.

the environmentally induced transformation, particularly on the microstructural aspects [11–13]. Furthermore, most papers on the degradation have been concerned with effects when the transformation was well advanced, i.e. when the transformation depth was tens of microns. This paper reports the results of an investigation of HIPped and hot pressed (designated unHIPped) bar samples of 3Y-TZP aged in an aqueous environment with and without the application of stress. HIPped femoral heads were used for the study of the effect of surface finish. The investigation concentrates on the early stages of the transformation, i.e. before the surface has totally transformed to monoclinic.

2. Experimental

The effect of stress was investigated using HIPped and unHIPped 3Y-TZP ceramic bar samples of nominal dimensions $30 \times 4 \times 3$ mm. All surfaces were finely polished to a roughness (R_a) of < 3 nm to eliminate any major flaws which might act as stress concentration sites. The mean grain size of the HIPped and unHIPped samples were 0.3 and 0.6 μm, respectively. In order to investigate whether stress affected degradation, three point bend testing was conducted at 89 ± 1 °C in double distilled water employing stresses in the range of 220–1226 MPa, and aging times of up to 800 h. The stresses quoted are the maximum tensile stresses.

The as-received condition of all samples was analyzed using both white light interferometry and glancing angle X-ray diffraction. Once three point bending had been completed, samples were again analyzed to investigate changes in the surface topography and ratio of monoclinic to tetragonal phases. In addition, scanning electron microscopy (SEM) analysis was also conducted on selected samples.

HIPped 32 mm diameter femoral heads with three surface finishes, namely rough, lapped and polished were also aged in double distilled water at 89 ± 1 °C for up to 1000 h and examined using the same characterization techniques as for the bars. All samples were supplied by Norton Desmarquest Fine Ceramics, France.

2.1. X-ray diffraction

A Philips X'Pert, materials research diffractometer (MRD) using Cu K_α radiation was used. The system was operated in thin film mode, facilitating the use of low incidence angles to determine both bulk phase content and transformation depth. This arrangement prevented radiation from penetrating as deeply below the sample surface compared to standard X-ray diffraction techniques. As a consequence surface layers could be analyzed, allowing the extent and depth of the transformation to be determined.

The depth (D) to which radiation penetrates into the 3Y-TZP ceramic is not a precise value but can be estimated by first calculating the path length (x) of the X-ray beam within the material. Substituting the mass absorption coefficient (μ), density (ρ), incident beam intensity (I_o) and transmitted beam intensity (I) into Equation 1, enables x to be determined. It was arbitrarily chosen to calculate the depth from which 99% of the information is derived, i.e. $I/I_o = 0.01$.

$$I = I_o \exp(-\mu\rho x) \tag{1}$$

Because of the asymmetric arrangement of the parallel beam optics, the relationship between D, the depth of penetration below the sample surface and Ω, the angle between the incident beam and the sample surface is given by

$$D = \frac{x}{(1/\sin\Omega) + (1/\sin(2\theta - \Omega))} \tag{2}$$

Ten different angles of omega were employed (2, 2.5, 3, 3.5, 4, 6, 8, 10, 12 and 14) and from the XRD patterns obtained the monoclinic content at each omega angle was calculated.

To determine the depth of the transformed layer a model was used based on the simple schematic in Fig. 1(a), where the cylinders represent monoclinic regions at the sample surface surrounded by the untransformed, tetragonal phase (subscripts t and m refer to tetragonal and monoclinic respectively). Using this model for the condition where X-ray penetration depth D is less than the depth of monoclinic phase below the surface L, it can be shown that the total volume fraction monoclinic in the interrogated volume is

$$V_m = \frac{C}{D} + C' \tag{3}$$

where C and C' are constants, $C = nA_m y$ (n is the number of monoclinic regions per unit area, A_m is the cross sectional area of the monoclinic cylinders and y the height of the monoclinic region above the tetragonal surface). When D is greater than L the total volume fraction monoclinic is

$$V_m = \frac{C''}{D} \tag{4}$$

where $C'' = nA_m(y + L)$ and is therefore greater than C. These two conditions are represented in Fig. 2 where

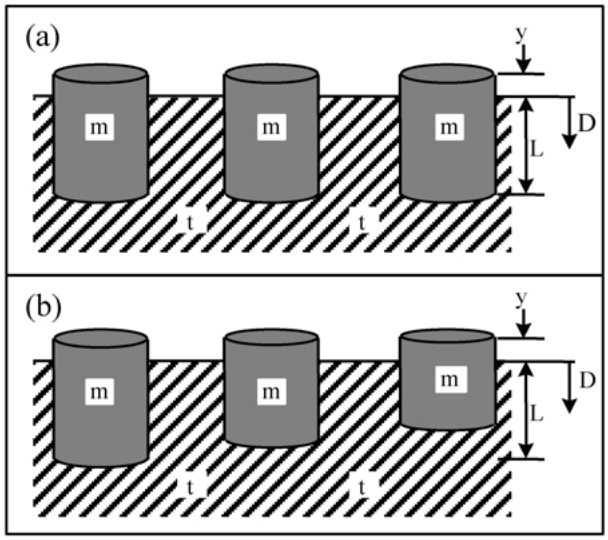

Figure 1 Schematic representation of transformation in a tetragonal matrix, (a) where the cylinders represent monoclinic regions of similar depths and (b) where there is variation in monoclinic depth (possible effect relating to applied stress).

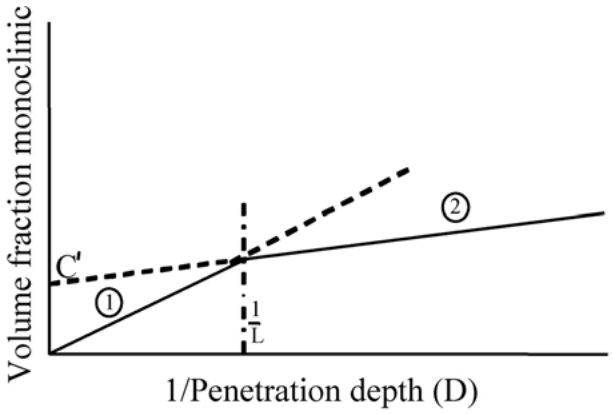

Figure 2 Displays linear region 1 where $D \geq L$ and linear region 2 where $D < L$.

volume fraction monoclinic is plotted against $1/D$. Region 1 corresponds to the condition described by Equation 4, where D is greater than L, and the line passes through the origin. The condition described by Equation 3, where D is less than L and the line has a lower gradient than for region 1 and does not pass through the origin, is represented by region 2. Thus the intercept of the two lines is at the point $D = L$.

This method of determining the transformation depth L does however have limitations. Depths below 2 μm could not be determined, as the lowest omega angle that was used for this work was 2°. The maximum angle used was 14° which corresponds to a maximum measurable transformation depth of 9.5 μm. This limitation relates to the glancing angle geometry, above 14° the angle formed approaches that of the Bragg focusing arrangement for the measured peaks.

The stress on the tensile face of a three point bend specimen is not constant and, if stress has an effect on the transformation, the depth of transformation might be expected to vary with position along the tensile face. This situation is represented in Fig. 1(b). In this case it can be shown that for $D \geq L$ an equation of the form of Equation 4 applies but with a different value for the constant which is determined by the rate of change of the depth of the monoclinic regions with position. For $D \leq L$ an equation similar in form to that of Equation 3 is obtained but with the constant C slightly varying with depth in a manner that depends on the change in depth of the monoclinic content with position. However, within normal experimental accuracy, it may be assumed that there is a linear relationship between V_m and D for $D \leq L$. Thus the analysis of the glancing angle X-ray data, represented in Fig. 2 is applicable to monoclinic depths that are constant (Fig. 1(a)) and vary (Fig. 1(b)) along the tensile face; in the latter the maximum depth of the monoclinic regions is determined.

The model and the analysis procedure are also applicable to studies of the compression face of the three point bend sample.

2.2. Surface interferometry

White light interferometry was used to analyze areas of 300×200 μm on the surface of all bar samples. Typically twelve measurements were recorded on both the compression and tension surfaces. For the femoral heads areas of 700×530 μm were monitored at six points around the head. It was necessary to mathematically compensate for a slight cylindrical effect caused by curvature on the sample surface. Three main images were recorded in each case; a contour plot, 3D plot and depth profile. These images were used to determine the size, frequency and form of the nuclei occurring on the sample surface during aging in double distilled water at 90 °C.

2.3. Scanning electron microscopy (SEM)

The SEM equipment was used to investigate surface topography. Analysis, conducted at various magnifications, required that the sample stage be tilted for surface features to be revealed. It was necessary to used an SEM fitted with a field emission gun to improve the resolution of small surface features. Only selected bar samples were studied.

3. Results and discussion

3.1. Effect of surface roughness

The monoclinic content calculated from the XRD patterns and the surface roughness, Ra, determined by white light interferometry are given for the femoral heads with the different surface finishes prior to testing in Table I. It can be seen that the rough surface finish is considerably rougher and has a higher monoclinic content than the lapped and polished finishes, which are more similar. In spite of these differences, which lead to differences in true surface area and probably stress state, there is little influence of the surface finish on the environmental degradation (Fig. 3).

The curves in Fig. 3 have characteristics which indicate a possible nucleation and growth process, hence the data was applied to a rearranged version of the Johnson-Mehl-Avrami equation:

$$\ln\,[-\ln(1 - X_m)] = \ln k + n \ln t \qquad (5)$$

where X_m is the monoclinic content as determined by X-ray diffraction, k is the linear intersect, n is the time exponent which varies between 1 and 4, and t is the aging time. Data obtained from long and short aging times can be misleading in that there is little change in the monoclinic content. Hence, only values between

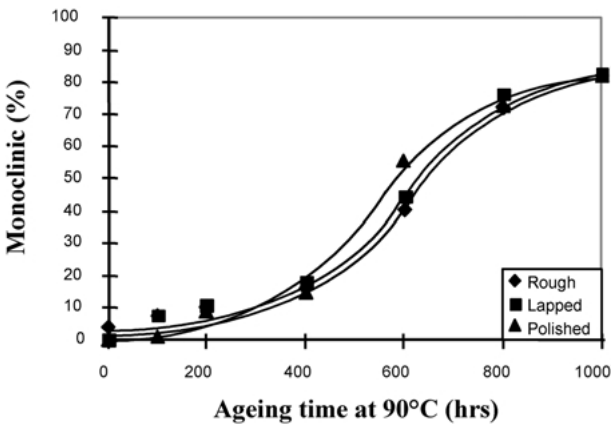

Figure 3 Graph showing that surface finish of femoral heads has a negligible effect on monoclinic content on aging in water at 89 ± 1 °C.

TABLE I Monoclinic content and surface roughness of the femoral heads with different surface finishes

	Rough	Lapped	Polished
Monoclinic (%)	5.2	1.7	0
Roughness (μm)	0.134	0.010	0.003

~ 400 and 800 h were considered even though this meant only three data points were used for each finish. A value of about 3.5 was obtained for all surface finishes; this is in reasonable agreement with the value of ~ 4, which is consistent with growth in three directions and a rate constant of 1, previously reported [7, 8].

The tetragonal to monoclinic transformation is accompanied by a volume change and consequently a transformed region appears as a small mound on the surface surrounded by flat regions of untransformed tetragonal phase. The transformation results in an increase in roughness as more monoclinic is formed up to an aging time of 800 h (Fig. 4). There is a slight fall in Ra at longer times due to the surface being almost completely transformed to monoclinic.

3.2. Comparison of HIPped and unHIPped samples

The bulk phase content was determined by X-ray diffraction in thin film mode at an Ω angle of 14°; the effect of time aging in water at 90 °C on the monoclinic content is shown in Fig. 5 for unstressed HIPped and unHIPped material. The monoclinic content increases more rapidly in the unHIPped samples due to the lower activation energy for transformation as a result of the larger grain size when compared with HIPped samples.

The time exponent n was determined from the HIPped data for times 400–800 h inclusive; a value of 3.6 was calculated, i.e. a similar value to that for the femoral heads with different surface finishes. It was not possible to calculate an n value for the unHIPped samples due to a lack of data points in the time region of greatest interest.

The transformation layer depths determined for both the HIPped and unHIPped samples have been plotted in Fig. 6. The values determined for the HIPped samples aged for up to 800 h, show an increase in the monoclinic layer depth with increasing aging time. A similar, but more rapid increase in layer depth with respect to increasing aging time is also evident for the unHIPped samples.

The depth of the monoclinic layer is greater than the grain size even though the complete surface has not been transformed to monoclinic. This compares favorably with the model based on optical interferometry proposed by Chevalier *et al*. [8] (Fig. 7). The diagram in Fig. 7(a) represents a cross-section through the material along the axis indicated in Fig. 7(b). The authors commented that the monoclinic content increased at a constant rate with time, based on transformation occurring in a conical configuration as a result of the initial transformed grain triggering transformation of the surrounding grains.

The plot of the number of nuclei per unit area as a function of aging time (Fig. 8) shows the expected increase in nuclei density with time for both the HIPped and unHIPped samples. The most significant difference lies in the incubation period prior to transformation; the unHIPped samples begin to transform at very short times whereas nucleation in the HIPped samples occurs only after aging for 200 h.

The rate of nucleation cannot be taken directly from Fig. 8, as it is necessary to correct the data for the decreasing amount of tetragonal phase available for transformation with time. A true nucleation rate of $7 \pm 5 \times 10^3\ m^{-2}s^{-1}$ was determined for both conditions but this value should not be relied upon too heavily due to the sparseness of data available. However, it appears that although the unHIPped samples begin to transform at earlier aging time than the HIPped samples there is not a concomitant increase in the true nucleation rate in the former.

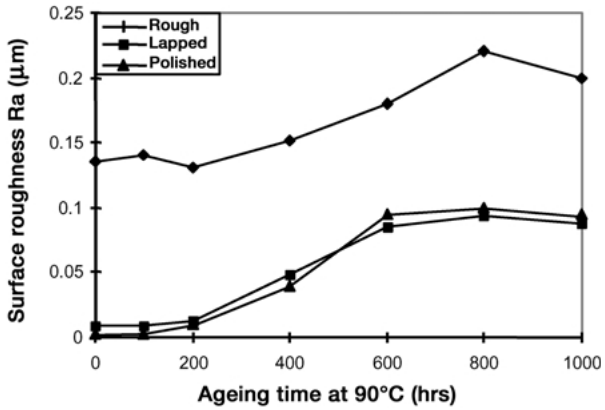

Figure 4 Change in surface roughness due to the tetragonal to monoclinic transformation for three surface finishes.

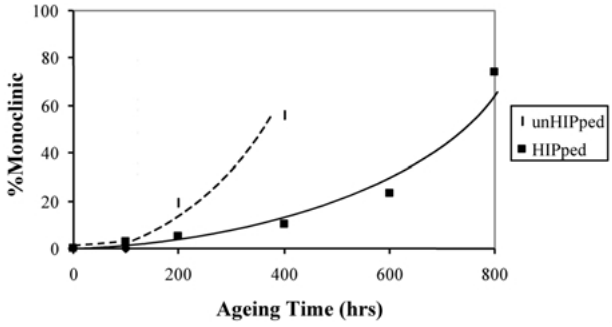

Figure 5 Comparison of monoclinic content following aging at 89 ± 1 °C for HIPped and unHIPped materials.

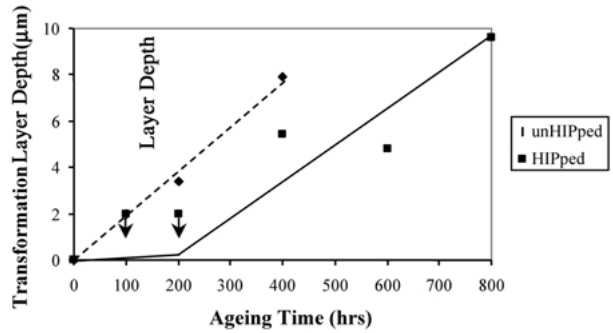

Figure 6 Monoclinic transformation layer depth against aging time for HIPped and unHIPped samples. Arrows on the figure indicate values of less than 2 μm.

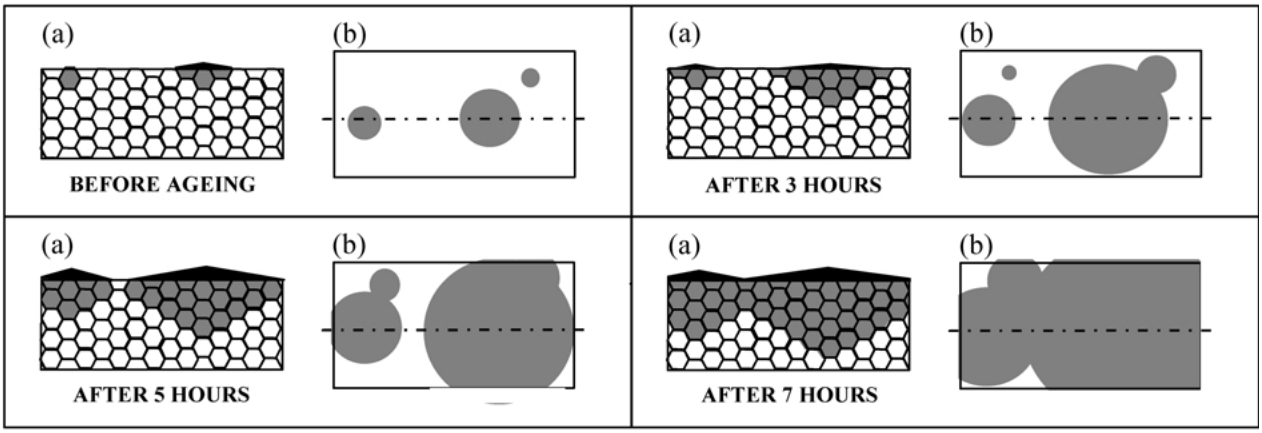

Figure 7 Model proposed by Chevalier *et al.* [8] for transformation in Y-TZP ceramics. The black mounds and grey regions indicate transformation above and below the surface, respectively.

The mean diameter of the largest nuclei in HIPped and unHIPped samples increases with aging time (Fig. 9). Comparison of the data reveals (i) different growth rates of 1.9×10^{-11} and $2.9 \times 10^{-11}\,\mathrm{ms}^{-1}$ for HIPped and unHIPped samples, respectively and (ii) a shorter incubation period for the unHIPped condition.

The determined true nucleation rate and the growth rates have been applied to the Johnson-Mehl-Avrami equation for constant nucleation and growth in three directions

$$X_m = 1 - \exp\left(-\frac{\pi}{3} G^3 I_v t^4\right) \tag{6}$$

where X_m is the monoclinic content, G is the growth rate, I_v is the nucleation rate per unit volume (to a reasonable approximation $I_v = I_a^2$, where I_a is the nucleation rate per unit area) and t is the aging time.

Fig. 10 compares the predicted monoclinic content with that determined by XRD for both the HIPped and unHIPped samples. Both predicted data (shown as a dotted line) and the experimental results indicate that for the unHIPped material the monoclinic content increases more rapidly and there is a shorter incubation period; in this respect the agreement between the predictions from white light interferometry data and X-ray diffraction results is encouraging. The discrepancy is attributed to the limited number of data points available and hence errors in the measured nucleation and growth rates. The predicted curves are sensitive to the values for G and I_v, for example the solid curve in Fig. 10 was produced by decreasing the true nucleation value by 25%; the result is an increase in the incubation period for the HIPped material and a more favorable agreement with the XRD data for both materials. Hence, it is important that further investigation be conducted to establish the nucleation and growth rates with a greater degree of accuracy.

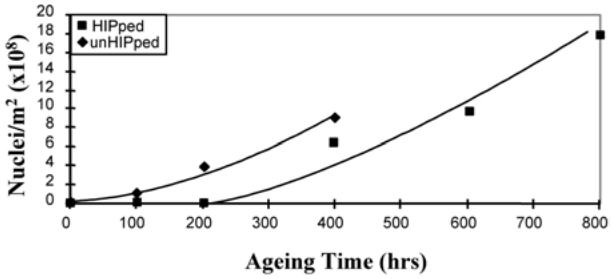

Figure 8 Nuclei/m^2 against aging time for both HIPped and unHIPped samples determined using white light interferometry.

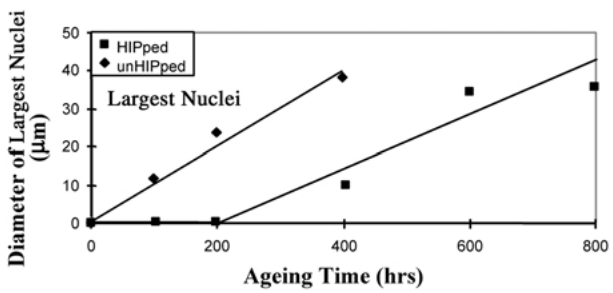

Figure 9 Diameter of largest nuclei against aging time for both HIPped and unHIPped samples determined using the ZYGO data.

3.3. Combined effect of aging and stress on HIPped and unHIPped samples

XRD analysis of samples subjected to stress showed a slight increase in monoclinic content with respect to the unstressed samples. For example, on aging for 400 h an increase of 12% monoclinic phase was recorded for HIPped samples subjected to an applied stress of 816 MPa while a 3% increase was found for unHIPped

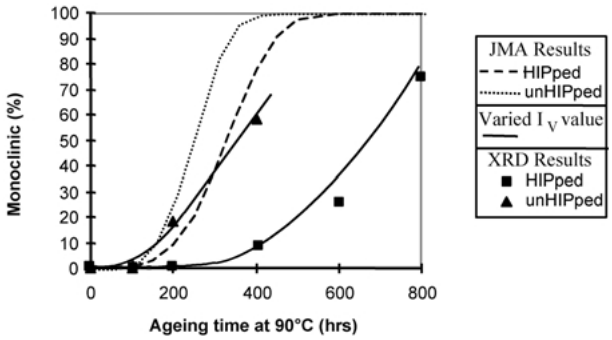

Figure 10 Comparison of monoclinic content determined using the JMA equation for nucleation and growth in three directions and XRD data. The dotted line was produced using determined values for true nucleation rate and growth rates and the full line by reducing the true nucleation rate value by 25%.

samples subjected to a maximum stress of 408 MPa for the shorter aging time of 200 h.

There is also an increase in the depth of the transformed layer with respect to stress (Fig. 11). For HIPped samples the depth of the monoclinic layer increased from 5.5 μm (for samples aged for 400 h at 90 °C, without stress) to 7 μm when a maximum stress of 816 MPa was applied for the same aging time. The unHIPped samples displayed an increase in the depth of the transformed layer with stress after only 200 h aging at 90 °C in water. When subjected to an applied stress of 408 MPa the depth of the monoclinic phase was found to be 8 μm; this is approximately 4.5 μm greater than was recorded for unstressed, unHIPped sample subjected to the same aging time.

The white light interferometry results demonstrated an increase in the number of nuclei, and hence the nucleation rate, with respect to stress for HIPped and unHIPped material. As may be seen from Fig. 12, the greatest increase occurred at longer aging times when subjected to the higher stresses, e.g. for HIPped samples aged for 400 h the number of nuclei increased from $6 \times 10^8\ m^{-2}$ for the unstressed condition to $15 \times 10^8\ m^{-2}$ under an applied stress of 816 MPa. A similar trend was shown by the unHIPped material which, for example, on aging for 200 h the density of nuclei was $4 \times 10^8\ m^{-2}$ in the unstressed condition compared to $8 \times 10^8\ m^{-2}$ when subjected to a maximum stress of 408 MPa. It was also observed that the diameter of the nuclei increase with increasing stress as exemplified by the results presented for the HIPped material in Fig. 13. Thus it may be concluded that stress enhances both nucleation and growth of the monoclinic phase.

White light interferometry analysis was used to investigate compression and tension surfaces. In all cases where the average number of nuclei on the two surfaces varied with position as shown in Fig. 14, it was found that more nuclei formed on the compression surface regardless of whether the material was HIPped or unHIPped.

Interestingly, a significant number of microcraters were observed, on the tension surface and most

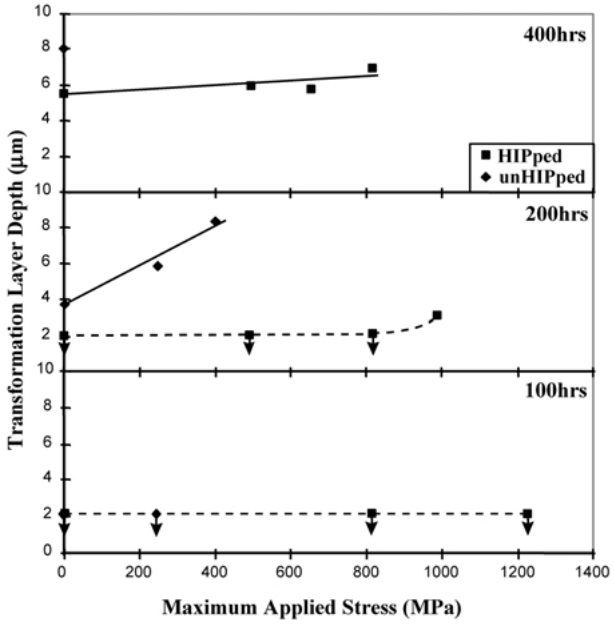

Figure 11 Comparison of the transformation layer depth of HIPped and unHIPped samples as a function of stress. Arrows on the figure indicate values of less than 2 μm.

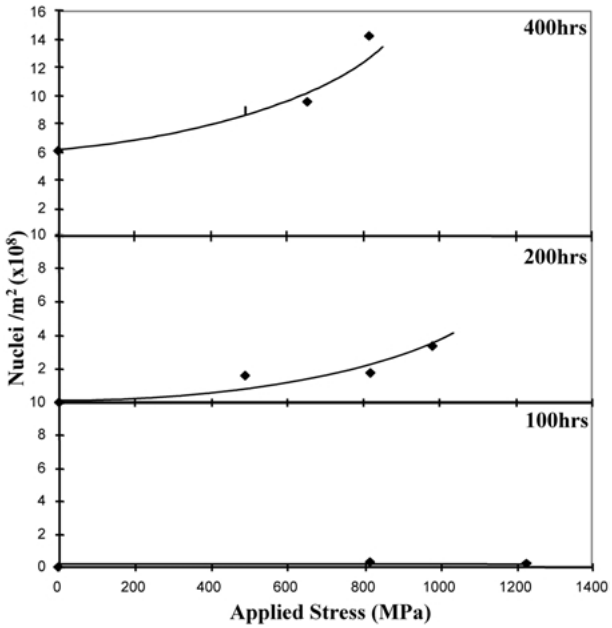

Figure 12 Effect of stress on the number of nuclei in HIPped material aged in water at 89 ± 1 °C.

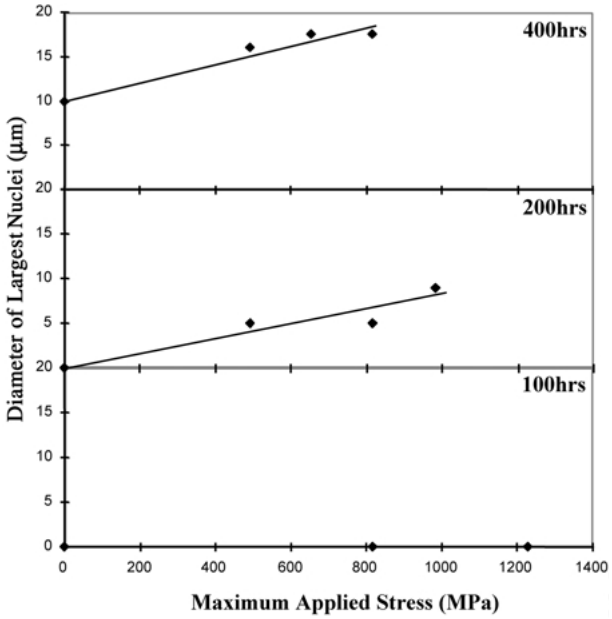

Figure 13 Effect of stress on the diameter of the nuclei in HIPped material aged in water at 89 ± 1 °C.

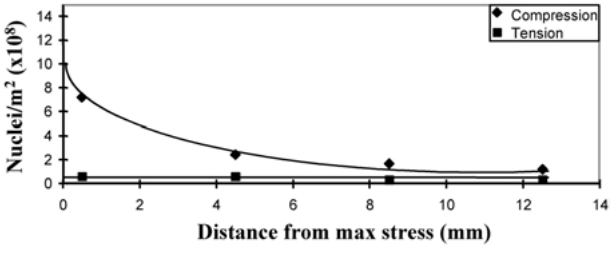

Figure 14 Comparison of the compression and tension surfaces of HIPped samples aged for 200 h under a maximum applied stress of 980 MPa.

frequently in the unHIPped samples – the number of microcraters was significantly less in the HIPped material. The microcraters most commonly appeared either next to, or within transformed regions (i.e. the mounds on the sample surface).

As yet one can only theorize as to why and/or how these microcraters form. The most likely possibility is that the craters were formed as transformed grains were ''flicked out'' of microcracked transformed regions under the action of an applied stress. A schematic representation of this scenario is shown in Fig. 15. Scanning electron microscopy images (Fig. 16) and depth profiling of such a microcrater using white light interferometry seems to confirm this explanation (Fig. 17).

3.4. Significance of the results

The results have clearly demonstrated the merits of employing HIPped, fine-grained 3Y-TZP rather than the larger grain sized hot-press material for biomedical applications such as the femoral head. However, the present results were acquired at 90 °C whereas body temperature is 37 °C. Applying the value for the activation energy for the environment induced transformation of 100 kJ mol^{-1} determined by Chevalier *et al.* [8], it can be predicted by using an Arrhenius type equation that in water at 37 °C the first nuclei would form

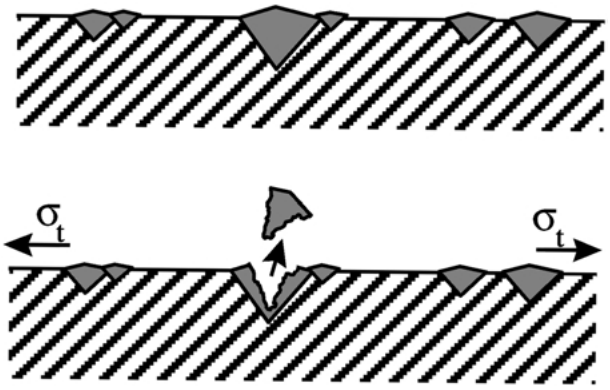

Figure 15 Possible mechanism for the formation of microcraters on the tension surface, where grains are ''flicked out'' of transformed regions.

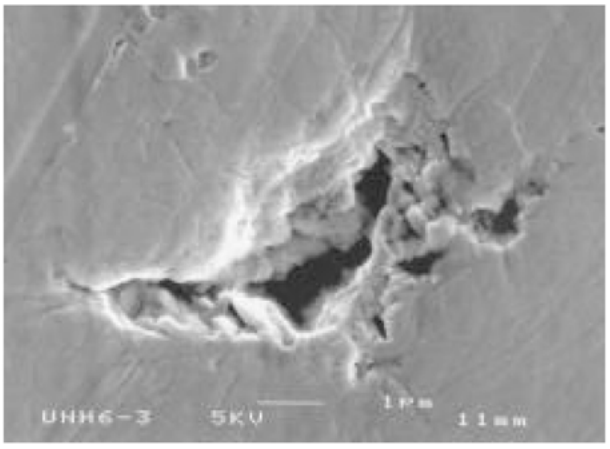

Figure 16 Displays a microcrater occurring at the center of a monoclinic mound, in an unHIPped sample aged for 200 h under a maximum applied stress of 245 MPa.

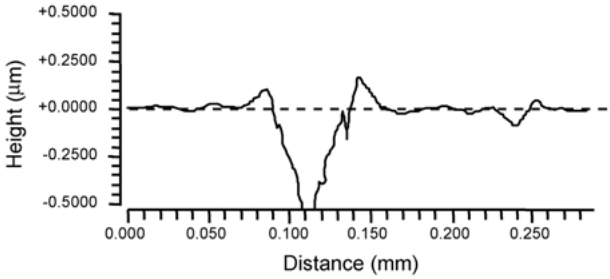

Figure 17 Depth profile, obtained using white light interferometry, through a microcrater.

on the surface of unstressed HIPped material after approximately 7 years. The time for nearly 100% transformation at the surface is, of course, much longer at in excess of 15 years.

This time period for the first nuclei would be reduced to about 5 years (assuming that stress does not change the activation energy) due to the effect of stress in enhancing the transformation. On the other hand, a major difference between the test and body environments is the presence of proteins in the latter. Polar proteins in the body fluid are attracted to the charge associated with the surface ions of Y-TZP. The proteins bind to the zirconia [14] and may consequently decrease the degradation rate. The predictions are therefore consistent with femoral heads explanted after two to three years showing no evidence of transformation.

The insensitivity of the environment induced transformation to the surface finish is an advantage as it permits some variation in finish without detriment to stability. In contrast, the effect of stress is a problem, not only through the enhancement of the transformation but also by causing the formation of microcraters on surfaces subject to a tensile stress. The microcraters are significant surface flaws and are potential sites for failure initiation. In addition articulation of flawed surfaces would lead to a decrease in wear resistance and an increase in debris. Zirconia debris can stimulate an adverse cellular reaction [15, 16] which, in extreme cases, may eventually lead to bone deterioration and loosening of the implant.

4. Conclusion

1. In the early stages of the transformation there was an increase in the depth of the monoclinic layer of both the HIPped and unHIPped materials with time even though the surface had not completely transformed to the monoclinic phase.

2. A true nucleation rate of $7 \pm 5 \times 10^3\,m^{-2}s^{-1}$ was determined for both HIPped and unHIPped conditions. The growth rate of unHIPped nuclei, $2.9 \times 10^{-11}\,ms^{-1}$ exceeds that of the HIPped nuclei $1.9 \times 10^{-11}\,ms^{-1}$. Application of these values to the JMA equation confirmed that unHIPped samples transform more readily and have shorter incubation periods prior to transformation than HIPped samples, although adjustment to values was required to obtain good agreement with the experimentally determined plot of monoclinic content against time.

3. The application of stress promotes an increase in the amount of transformed phase compared to unstressed

samples subjected to the same aging conditions. The transformation occurs more readily on the compression surface of samples under stress, while the tension surface (particularly of unHIPped samples) is prone to the formation of microcraters believed to result from expulsion of monoclinic grains from microcracked transformed regions.

Acknowledgments

One of the authors (KLG) is indebted to Norton Desmarquest Fine Ceramics and Howmedica for financial support. Stimulating discussions with B. Cales, F. Villermaux and C. Doyle are gratefully acknowledged.

References

1. R. STEVENS, *Proceedings of the first European Symposium on Engineering Ceramics*, Oyez Scientific & Technical Services Ltd. and Authors (1985).
2. W. M. KRIVEN, W. L. FRASER and S. W. KENNEDY, *Adv. Ceram.* **3** (1981).
3. M. WATANABE, S. LIO and I. FUKUURA, *Adv. in Ceram.* **12** (1984) 391.
4. M. YOSHIMURA, T. NOMA, K. KAWABATA and S. SOMIYA *J. Mat. Soc. Lett.* **6**(4) (1987) 465.
5. T. SATO and M. SHIMADA, *J. Am. Soc.* **67**(10) (1984) C212–213.
6. T. SATO and M. SHIMADA, *J. Am. Ceram.* **68**(6) (1985) 356–359.
7. K. L. GRANT and R. D. RAWLINGS, *J. Mat. Sci. Letts.* **18** (1999) 739–741.
8. J. CHEVALIER, B. CALES and J. M. DROUIN, *J. Am. Ceram. Soc.* **82**(8) (1999) 2150–2154.
9. I. THOMPSON and R. D. RAWLINGS, *Biomaterials* **11** (1990) 505–508.
10. B. CALLES and Y. STEPHANI, *J. Mat. Sci*: *Mat. Med.* **5** (1994) 376–379.
11. M. MATSUI, T. SOMA and I. ODA, *J. Mat. Ceram. Soc.* **69**(3) (1986) 198–202.
12. H. SCHUBERT, *Zirconia Ceramics* **7** (1986) 65–81.
13. A. HEUER, *J. Am. Ceram. Soc.* **70**(10) (1987) 689–698.
14. J. MEI, Ph.D. thesis, University of Birmingham (1997).
15. S. LEROUGE, L. H. YAHIA, O. HUK and SEDEL, ''Bioceramics'', edited by J. Wilson, L. Hench and D. Greenspan (Pergamon Press, 1995).
16. P. A. REVELL, in ''Bioceramics'', edited by J. Wilson, L. Hench and D. Greenspan (Pergamon Press, 1995).

Received 28 August
and accepted 1 November 2000